AAS 16-439

ORBITAL STABILITY REGIONS FOR HYPOTHETICAL NATURAL SATELLITES OF 101955 BENNU (1999 RQ_{36})

Samantha Rieger,[*] Daniel Scheeres[†] and Brent Barbee[‡]

The Origins, Spectral Interpretation, Resource Investigation, Security-Regolith Explorer (OSIRIS-REx) mission will be orbiting and returning a sample form near-Earth asteroid 101955 Bennu. Ground-based observations have determined that no object greater than 15 m in diameter is orbiting Bennu. This investigation explores the possible size and stability of a natural satellite around Bennu. The focus of this research is solely on the existence of stable orbits for a natural satellite and purposefully places how the natural satellite migrated to this orbit outside the bounds of this research. Numerical simulations modeling J_2, third body dynamics and solar radiation pressure is used on a large set of initial conditions that vary in semi-major axis, inclination, longitude of periapsis and natural satellite diameter. Stable orbital initial conditions for a given natural satellite diameter must remain in orbit for more than a thousand years without escape or collision from Bennu. The data found the possible existence of natural satellites in orbit around Bennu as small as 0.75 cm. Certain mechanisms such as the modified Laplace plane, Kozai resonance and the Sun-terminator plane are explored for yielding stable orbits of a given natural satellite.

INTRODUCTION

The Origins, Spectral Interpretation, Resource Investigation, Security-Regolith Explorer (OSIRIS-REx) mission to return a sample from potentially hazardous near-Earth asteroid (NEA) 101955 Bennu (1999 RQ_{36}) will become NASA's third New Frontiers Class mission when it launches in September of 2016. During its time at Bennu, the spacecraft will occupy two distinct Sun-terminator plane orbits: one at a radius of 1 km, and another at a radius of 1.5 km. Therefore, the mission planning team is currently investigating whether Bennu might possess any natural satellites in long-term stable orbits that could interfere with spacecraft operations in Bennu's vicinity. Bennu has been the target of an extensive ground-based observation campaign since its discovery in 1999, and those observations have ruled out the presence of any natural satellites larger than 15 m in diameter.[1,5]

To investigate whether stable orbits exist for $<$15 m natural satellites of Bennu, we vary initial conditions for semi-major axes, inclinations and longitude of the ascending nodes to find a range of possible orbits that are stable. Eccentricity will not be varied as an initial condition, but with perturbations from the Sun the eccentricity may increase significantly. Semi-major axes from 1 km out to the Hill sphere will be analyzed, since highly eccentric orbits may exist that bring the

[*] Graduate Student, Department of Aerospace Engineering Sciences, University of Colorado at Boulder, 431 UCB, Boulder, Colorado 80309, U.S.A. E-mail: samantha.rieger@colorado.edu.
[†] Professor, Department of Aerospace Engineering Sciences, University of Colorado at Boulder, 429 UCB, Boulder, Colorado 80309, U.S.A. E-mail: scheeres@colorado.edu.
[‡] Flight Dynamics Engineer, NASA/GSFC, Code 595, 8800 Greenbelt Road, Greenbelt, Maryland 20771, U.S.A. E-mail: brent.w.barbee@nasa.gov.

natural satellites very close to the surveying orbits of OSIRIS-REx. These initial conditions will be repeatedly evaluated for multiple sized satellites up to 15 meters in diameter. Each initial condition is simulated for 1000 years or until the natural satellite escapes or collides with Bennu. If there is escape or collision, these initial conditions are considered unstable. The ultimate end goal of this research is to determine orbits that are stable indefinitely or for 10,000's years. If a natural satellite is to exist at Bennu during the OSIRIS-REx arrival, it is more likely that it will be in an orbit that is stable for a 100,000 years as opposed to 900 years. However, sweeping through as many possible initial orbit conditions at Bennu for 10,000 to 100,000 years is computationally exhaustive. Therefore, 1000 years was a compromise to determine a preliminary idea of where such long term orbits exist. Typically most orbits that are stable for 1000 years are stable for 10,000 years, however there are exceptions. Some special test cases are simulated for 10,000 years to demonstrate the possibility of becoming unstable after 10,000 years or not.

There are some possible stable orbits that we expect to exist for varying diameter satellites. The first possible stable region will be due to the modified Laplace plane. The second is the Kozai resonance. The classical Laplace plane is normal to the axis about which the pole of a satellite's orbit precesses.[12] The modified Laplace plane includes Solar Radiation Pressure (SRP) perturbations, J_2 non-spherical gravity perturbations, and solar gravity.[7] In previous research, we have already determined some characteristics of the modified Laplace plane around Bennu.[6] First is that the modified Laplace plane becomes less stable as the distance between the satellite and primary increases. The modified Laplace plane is also less stable as the diameter of the satellite decreases.

The Kozai resonance is caused by third body perturbations on a satellite. This resonance causes libration of the satellite's argument of periapsis. This libration causes an exchange between eccentricity and inclination in such a way that the satellite's angular momentum in the Sun-Bennu orbit plane is conserved.[2]

Finally, an orbit can be stable for a natural satellite if on the Sun-terminator plane. A terminator plane orbit exists near a polar orbit with respect to the equator of the asteroid. These orbits tend to stay frozen in the Keplerian orbital elements except the longitude of the ascending node, which will precess at a rate equivalent with Bennu's orbit around the Sun.[10]

By constructing and executing an array of detailed simulations modeling the evolution of Bennu natural satellite orbits over thousand-year time scales, we will assess the possible sizes, orbital locations, and longevities of Bennu natural satellites. We note that theories proposing credible mechanisms for the in-situ formation or capture of such natural satellites are also required, but those studies are purposely placed outside the scope of our dynamical investigations. From these data we will draw conclusions about the likelihood of Bennu possessing natural satellites either in the past or during the current epoch, whether such natural satellites might interfere with OSIRIS-REx spacecraft operations around Bennu, and whether there are specific regions in the vicinity of Bennu within which the OSIRIS-REx team may wish to focus their efforts to search for <15 m natural satellites during the spacecraft's gradual approach to Bennu.

MODEL

Numerical Equations of Motion

Third Body Perturbations: The equations of motion are in the inertial Bennu orbit-centered frame. These equations can be derived using Newtonian mechanics from the equation

$$\boldsymbol{F} = m\boldsymbol{a}. \tag{1}$$

Where $\boldsymbol{F}$ is the force vector, $\boldsymbol{a}$ is an acceleration vector of mass m. It is assumed that the mass of the natural satellite is negligible such that it does not have an effect on Bennu's orbit. This gives the equation

$$\ddot{\boldsymbol{r}}_p = \frac{\mu_s}{|\boldsymbol{r}_s|^3}\boldsymbol{r}_s - \frac{\mu_s}{|\boldsymbol{r}_{sp}|^3}\boldsymbol{r}_{sp} - \frac{\mu_a}{|\boldsymbol{r}_p|^3}\boldsymbol{r}_p. \tag{2}$$

where μ_s is the gravitational parameter or the Sun, μ_a is the gravitational parameter of the Bennu, $\boldsymbol{r}_s$ is the distance from the asteroid to the Sun, $\boldsymbol{r}_p$ is the distance from the asteroid to the point-mass or satellite, and $\boldsymbol{r}_{sp}$ is the distance from the Sun to the point-mass/satellite. The above equation is the sum of the two-body motion between the satellite and the asteroid and the third body perturbations. Therefore just the third body perturbations are

$$\boldsymbol{a}_{sun} = \frac{\mu_s}{|\boldsymbol{r}_s|^3}\boldsymbol{r}_s - \frac{\mu_s}{|\boldsymbol{r}_{sp}|^3}\boldsymbol{r}_{sp}. \tag{3}$$

J_2 Perturbations: The second perturbation on the spacecraft is the J_2 perturbation from the asteroid. $J_2 = -C_{20}$, where C_{20} can be determined by

$$C_{20} = \frac{1}{5r_0}\left(\gamma^2 - \frac{\alpha^2+\beta^2}{2}\right), \tag{4}$$

where α is the asteroid's semi-major axis, β is the asteroid's semi-intermediate axis, γ is the asteroid's semi-minor axis, and r_0 can be defined as the mean radius or the maximum radius of the asteroid. For this analysis, r_0 is the maximum radius of the asteroid. The potential due to this perturbation is[11]

$$R_2(\boldsymbol{r}_p) = -\frac{\mu_a}{2|\boldsymbol{r}_p|^3}C_{20}R_a^2[1 - 3(\hat{\boldsymbol{r}}_p \cdot \hat{\boldsymbol{p}})^2]. \tag{5}$$

where $\hat{\boldsymbol{p}} = [0,\ \sin\epsilon,\ \cos\epsilon]$, or the spin pole of the asteroid in the asteroid orbit-frame. $R_2 = U - \frac{\mu}{r}$ and $\ddot{r} = \frac{\partial U}{\partial r}$, therefore the partial derivative of the potential will give the acceleration due to J_2.[11] To find the acceleration of R_2, first the equation can be rewritten as

$$R_2(\boldsymbol{r}_p) = -\frac{\mu_p}{2|\boldsymbol{r}_a|^3}C_{20}R_a^2[1 - \frac{3(\boldsymbol{r}_p \cdot \hat{\boldsymbol{p}})^2}{|\boldsymbol{r}_p|^2}]. \tag{6}$$

The partial derivative of the potential is

$$\frac{\partial U}{\partial \boldsymbol{r}_p} = \frac{3}{2}\frac{\mu_a}{|\boldsymbol{r}_p|^5}C_{20}R_a^2\left(1 - \frac{3}{|\boldsymbol{r}_p|^2}\left(\boldsymbol{r}_p \cdot \hat{\boldsymbol{p}}\right)^2\right)\boldsymbol{r}_p - \frac{\mu_a}{|\boldsymbol{r}_p|^3}C_{20}R_a^2\left(\frac{6}{|\boldsymbol{r}_p|^4}(\boldsymbol{r}_p \cdot \hat{\boldsymbol{p}})^2\right)\boldsymbol{r}_p. \tag{7}$$

With some simplification this equation becomes

$$\boldsymbol{a}_{J_2} = \frac{\partial U}{\partial \boldsymbol{r}_p} = \frac{3}{2}\frac{\mu_a}{|\boldsymbol{r}_p|^5}C_{20}R_a^2\boldsymbol{r}_p - \frac{15}{2}\frac{\mu_a}{|\boldsymbol{r}_p|^7}C_{20}R_a^2\left(\boldsymbol{r}_p \cdot \hat{\boldsymbol{p}}\right)\boldsymbol{r}_p + 3\frac{\mu_a}{|\boldsymbol{r}_a|^5}C_{20}R_a^2\left(\boldsymbol{r}_p \cdot \hat{\boldsymbol{p}}\right)\hat{\boldsymbol{p}}. \tag{8}$$

Solar Radiation Pressure Perturbations The final perturbation to be included is SRP. A simple Cannonball model will be used.[7]

$$\boldsymbol{a}_{SRP} = -(1+\rho)\frac{P_\Phi}{r_s^2 b}\hat{\boldsymbol{r}}_s, \tag{9}$$

where ρ is the reflectance, b, or m/A, is the mass-to-area ratio in kg/m^2, and P_Φ is the solar radiation constant and is approximately 1×10^8 km^3/s^2/m^2.[7]

Equations of Motion The equations of motion used for the numerical analysis is the sum of the perturbations and the two-body motion.

$$\boldsymbol{a} = -\frac{\mu_a}{|\boldsymbol{r}_p|^3}\boldsymbol{r}_p + \boldsymbol{a}_{sun} + \boldsymbol{a}_{J_2} + \boldsymbol{a}_{SRP} \tag{10}$$

The equation of motion is

$$\begin{aligned}\ddot{\boldsymbol{r}}_p = -\frac{\mu_a}{|\boldsymbol{r}_p|^3}\boldsymbol{r}_p + \frac{\mu_s}{|\boldsymbol{r}_s|^3}\boldsymbol{r}_s - \frac{\mu_s}{|\boldsymbol{r}_{sp}|^3}\boldsymbol{r}_{sp} + \frac{3}{2}\frac{\mu_a}{|\boldsymbol{r}_p|^5}C_{20}R_a^2\boldsymbol{r}_p - \frac{15}{2}\frac{\mu_a}{|\boldsymbol{r}_p|^7}C_{20}R_a^2\left(\boldsymbol{r}_p\cdot\hat{\boldsymbol{p}}\right)\boldsymbol{r}_p \\ +3\frac{\mu_a}{|\boldsymbol{r}_p|^5}C_{20}R_a^2\left(\boldsymbol{r}_p\cdot\hat{\boldsymbol{p}}\right)\hat{\boldsymbol{p}} - (1+\rho)\frac{P_\Phi}{r_s^2 b}\hat{\boldsymbol{r}}_s.\end{aligned} \tag{11}$$

Averaged Equations of Motion

The numerical equations of motion will be compared to the averaged equations of motion in some instances for the results. Some stable orbits will exist due to the modified Laplace plane, which is derived from the averaged equations of motion. The equations of motion are the rate of change of the Lagrange planetary equations of the Milankovitch orbital elements. These equations are integrated over time and therefore is independent of time or are secular. For these equations the perturbation from the Sun, J_2 and SRP is determined by a strength factor. These perturbation factors are measured by[7]

$$\begin{aligned}\omega_2 &= \frac{3nJ_2R_a^2}{2a^2}, \\ \omega_s &= \frac{3\mu_s}{4na_s^3h_s^3}, \\ \omega_{srp} &= \frac{2\pi(1-\cos\Lambda)}{T_s\cos\Lambda};\end{aligned} \tag{12}$$

where Λ is the SRP perturbation angle defined as

$$\tan\Lambda = \frac{3(1+\rho)P_\Phi}{2bV_{lc}H_s}. \tag{13}$$

When Λ goes to 0, the solar radiation pressure is weak and when Λ goes to $\pi/2$, SRP is strong.[7]

The averaged equations of motion use these perturbation factors. These equations are determined by the Lagrange Planetary Equations of the Milankovitch orbital elements.[8] The averaged equations of motion are just simply the sum of the averaged equations for each individual perturbation.[7]

$$\dot{\boldsymbol{h}} = -\frac{\omega_2}{h^5}\left(\hat{\boldsymbol{p}}\cdot\boldsymbol{h}\right)\tilde{\hat{\boldsymbol{p}}}\cdot\boldsymbol{h} - \omega_s\hat{\boldsymbol{H}}_{\boldsymbol{s}}\cdot\left(5\boldsymbol{e}\boldsymbol{e}^T - \boldsymbol{h}\boldsymbol{h}^T\right)\cdot\tilde{\hat{\boldsymbol{H}}}_{\boldsymbol{s}} - \omega_{srp}\tilde{\hat{\boldsymbol{H}}}_{\boldsymbol{s}}$$

$$\dot{\boldsymbol{e}} = -\frac{\omega_2}{2h^5}\left\{\left[1-\frac{5}{h^2}\left(\hat{\boldsymbol{p}}\cdot\boldsymbol{h}\right)^2\right]\tilde{\boldsymbol{h}} + 2\left(\hat{\boldsymbol{p}}\cdot\boldsymbol{h}\right)\tilde{\hat{\boldsymbol{p}}}\right\}\cdot\boldsymbol{e} \tag{14}$$

$$-\omega_s\left[\hat{\boldsymbol{H}}_{\boldsymbol{s}}\cdot\left(5\boldsymbol{e}\boldsymbol{h}^T - \boldsymbol{h}\boldsymbol{e}^T\right)\cdot\tilde{\hat{\boldsymbol{H}}}_{\boldsymbol{s}} - 2\tilde{\boldsymbol{h}}\cdot\boldsymbol{e}\right] - \omega_{srp}\tilde{\hat{\boldsymbol{H}}}_{\boldsymbol{s}}\cdot\boldsymbol{e} \tag{15}$$

Where the angular momentum vector is normalized by $\boldsymbol{h}/\sqrt{\mu_p a}$.[7] This gives non-dimensional equations of motion.

Circular Laplace Equilibria For the current analysis, it will be assumed that the satellite is in a circular orbit about the asteroid. This suggests that $\dot{\boldsymbol{e}} = 0$ in Equation (15). For this equilibrium analysis, we will also assume the SRP terms in Equation (15) are also zero. This gives the equilibrium equation[12]

$$\omega_2\left(\hat{\boldsymbol{p}}\cdot\hat{\boldsymbol{h}}\right)\tilde{\hat{\boldsymbol{p}}}\cdot\hat{\boldsymbol{h}} + \omega_s\left(\hat{\boldsymbol{H}}_{\boldsymbol{s}}\cdot\hat{\boldsymbol{h}}\right)\tilde{\hat{\boldsymbol{H}}}_{\boldsymbol{s}}\cdot\hat{\boldsymbol{h}} = 0. \tag{16}$$

This equilibrium can be put in terms of the obliquity and Laplace angle, such that the Laplace angle can explicitly be solved.[12]

$$\omega_2\sin 2\phi + \omega_s\sin 2(\phi-\epsilon) = 0 \tag{17}$$

The Laplace angle ϕ is an azimuthal angle measured from the body's spin axis.[7] This angle will define the orbit to lie in-between the equator and the orbital plane such that as a goes to 0, ϕ goes to 0 and when a goes to ∞, ϕ goes to ϵ. There exists a Laplace radius, which defines the semi-major axis of the trajectory where the Laplace equilibria bisects the angle between the equator and the orbital plane. The Laplace radius is defined as[12]

$$r_L^5 = 2J_2R_a^2a_s^3\left(1-e_s^2\right)^{3/2}\frac{m}{m_s}. \tag{18}$$

Modified Laplace Equilibria With the inclusion of the SRP perturbation terms in Equation (15), the Laplace equilibrium is now[7,9]

$$\omega_2\left(\hat{\boldsymbol{p}}\cdot\hat{\boldsymbol{h}}\right)\tilde{\hat{\boldsymbol{p}}}\cdot\hat{\boldsymbol{h}} + \omega_s\left(\hat{\boldsymbol{H}}_{\boldsymbol{s}}\cdot\hat{\boldsymbol{h}}\right)\tilde{\hat{\boldsymbol{H}}}_{\boldsymbol{s}}\cdot\hat{\boldsymbol{h}} + \omega_{srp}\tilde{\hat{\boldsymbol{H}}}_{\boldsymbol{s}}\cdot\hat{\boldsymbol{h}} = 0. \tag{19}$$

In terms of obliquity and the Laplace angle the equilibrium is[7,9]

$$\omega_2\sin 2\phi + \omega_s\sin 2(\phi-\epsilon) + 2\omega_{srp}\sin(\phi-\epsilon) = 0. \tag{20}$$

The Laplace Angle increases for the same radii as the SRP increases. We are assuming that $\rho = 0$ and we will compare mass-to-area ratios of $b = 100\ kg/m^2$, $b = 1000\ kg/m^2$, and no SRP. The

difference can be seen in Figure 1. For reference, a natural satellite with a mass-to-area ratio of 100 kg/m^2 and 1000 kg/m^2 is 0.075 m and 0.75 m respectively. A mass-to-area ratio of 0 kg/m^2 is the same as a point-mass, since there is no area in which SRP can be applied using the Cannon ball model.

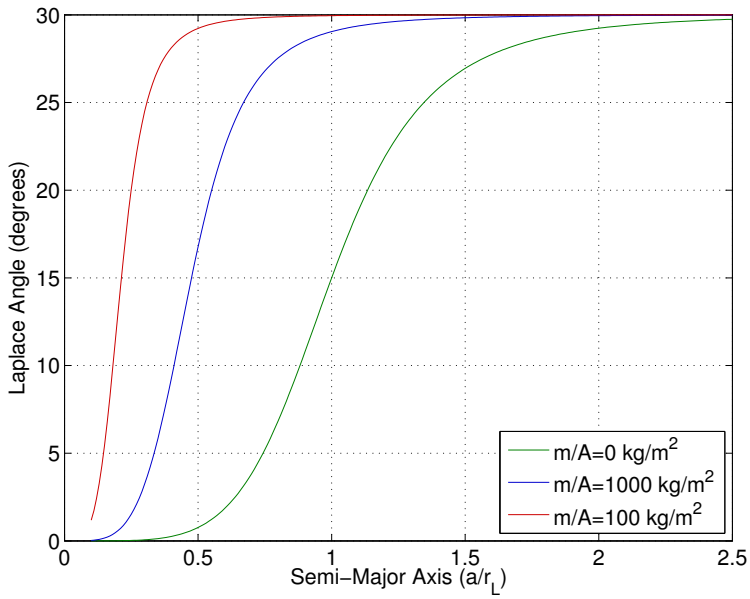

Figure 1. The Laplace angle as a function of semi-major axis normalized by the Laplace radius is shown above for mass-to-area ratios of 0, 100, 1000 kg/m^2 at Bennu. For $b = 0\ kg/m^2$, the Laplace radius is equivalent to 1 at the bisection of the obliquity ($30°$) such that the Laplace angle is $15°$. For an increase in the mass-to-area ratio the bisection occurs at a smaller semi-major axis.

Kozai Resonance For a Kozai resonance to occur, the satellite has negligible mass compared to the other two bodies in a three body system, with the distance between the primary, Bennu, and the satellite being much closer than that of the primary to the Sun. These are both true in this scenario. A Kozai resonance is caused by the orbit's argument of periapsis librating due to perturbations from the Sun. Using the average equations of motion for just third body dynamics, their is a conserved quantity, which is the angular momentum of the satellite's orbit in the Sun-Bennu orbit plane. This can be quantified as:

$$H_z = \sqrt{(1 - e^2)} \cos i \tag{21}$$

Therefore the eccentricity and inclination of the satellites orbit will vary, as inclination increases the eccentricity will decrease and vice versa. The Kozai resonance will most likely occur further out from the asteroid such that spherical harmonics will not significantly perturb the system. The satellite will also have to be large enough to not be perturbed significantly from SRP. Also, it should be noted that at certain inclinations, particularly high inclinations, the Kozai resonance will cause instability since the eccentricity will be too large. Eccentricity will increase such that it will result in a collision with Bennu or escape outside of the Hill sphere at its apoapsis.

Sun-Terminator Plane In order to determine if the terminator plane is causing the orbit to be stable, the longitude of periapsis must precess at the same rate that Bennu travels around the Sun. Bennu's period is 436.6487279241047 days.[1] Therefore, the rate of precession for the longitude of the ascending node must be equivalent to:

$$Rate = \frac{360^\circ}{1.19629788472357\ years} = 300.928393000698\ deg/year \tag{22}$$

Implementation

To help characterize and understand the orbits of possible natural satellites, the parameters to be studied will be the semi-major axis of the satellite's orbit, diameter of the satellite, and the time the orbit remains stable. All parameters for Bennu will be held constant. The parameters used in this research are listed in Table 1.[1,3,5]

Table 1. Bennu Parameters

Parameter	Value
Obliquity (with respect to the orbit plane of Bennu), ϕ	176°
Gravitational parameter, μ_a	5.2 m^3/s^2
Assumed density of Bennu satellites , ρ	2 kg/m^3
Body Major Axis, α	567 m
Body Intermediate Axis, α	535 m
Body Minor Axis, α	508 m
Orbit Semi-Major axis, a_s	1.126391025996 AU
Orbit Eccentricity, e_s	0.203745112
Orbit Inclination, i_s	6.0349391°
Orbit Arg. of Periapsis, w_s	2.0608668°

It should be noted that the assumed density of Bennu's satellites are larger than the defined density for Bennu. Bennu is a rubble pile and therefore may have space between the boulders and rocks that comprise it, while the natural satellite will either be a boulder itself or much denser than Bennu. With the assumed value of 2 kg/m^3 for the density of the natural satellites, we can now determine approximately the size of the natural satellite. Assuming the natural satellite is a sphere, the SRP will only hit one side and thus the area of a circle will be in the Sun direction. The mass-to-area ratio will have the area of a circle substituted in for area.

$$\frac{m}{a} = \frac{m}{\pi r^2} = b \tag{23}$$

The equation for a mass of an object knowing the density and volume is

$$m = \rho v = \frac{4}{3}\rho\pi r^3, \tag{24}$$

where the volume can be substituted with with volume of a sphere. Then set mass equal two each other from equation (23) and (24).

$$\pi r^2 b = \frac{4}{3}\rho\pi r^3 \tag{25}$$

The radius of the natural satellite is:

$$r = \frac{3}{4}\frac{b}{\rho} \tag{26}$$

Thus, the diameter is:

$$D = \frac{3}{2}\frac{b}{\rho} \tag{27}$$

The semi-major axes studied are from orbits of 1 km out to the Hill sphere, this will include any orbits that grows in eccentricity that may intersect with the OSIRIS-REx survey orbits. The mass-to-area ratios will be from the minimum mass-to-area ratio to yield a stable orbit to 20,000 kg/m^2. For the density we are assuming, this will be up to a 15 m diameter satellite. Finally, the actual density of these satellites can vary from the assumed value, so the diameters given are approximate.

Depending on the rotation of the satellite, the size can be further constrained. According to D. S. Lauretta, et. al., a 15 meter object will have a rotation period of 1 min, while a 5 m satellite will have a period of 1 hour and a 2 m object will have a rotation period of 24 hours.[5] The time for the majority of runs will be 1000 years. This is ample time to preliminarily determine orbits that can be stable for long enough that it is possible a satellite will be there when OSIRIS-REx arrives. But also, short enough that computations are not overly time-consuming. However, there will be case studies on several examples with larger time scales to determine how this changes the results. Finally, for the natural satellite around Bennu, it is assumed that the initial orbit is always circular for simplicity of the study. Future work will explore a range of eccentricities, since eccentricity can cause certain orbits to become more stable.[10]

The initial conditions tested will be at semi-major axes of 1 km, 2 km, 3 km, 4km, 5 km, 10 km, 15 km, 20 km, 25 km, and 30 km. For each semi-major axis the mass-to-area ratios between 1000 kg/m^2 to 10,000 kg/m^2 in intervals of 1000 kg/m^2 will be tested. This covers a range of natural satellites from 0.0075 to 15 m. in diameter. If 1000 kg/m^2 has stable orbits for 1000 years, then smaller diameters with be examined as well. First, 100 to 900 kg/m^2 in intervals of 100 kg/m^2, and then 10 to 90 kg/m^2 in intervals of 10 kg/m^2 if 100 kg/m^2 yields stable orbits. For any given semi-major axis and mass-to-area ratio, 120 iterations of varying initial conditions are integrated for 1000 years. The 120 iterations vary with $\Omega = 0^\circ\ , 90^\circ\ , 180^\circ\ , 270^\circ$ and inclination from 0° to 180° in increments of 6 degrees. This is a lot of data and cannot all be displayed in this paper, therefore the results will give examples and best summarize the noticeable trends within the data.

RESULTS

A summary of the full results can be seen in Tables 2 and 3. The two tables give a list of all diameters a natural satellites that are stable for 1000 years at a given inclination and semi-major axis. It is important to note that often there are bands of stable diameters. For instance in Table 2 at a semi-major axis of 2 km and an inclination of 54° the diameters that are stable are $0.03 - 0.06$ m and $1.5 - 15$ m. These ranges of diameters are both stable for two different reasons. As will be discussed below, the smaller ranges of diameters for natural satellites are usually stable because of the terminator plane.

Table 2. Range of stable natural satellite diameters for semi-major axes 1-5 km.

	Semi-major axis (km)				
	1	2	3	4	5
i°	Diameter (m)				
0	0.3-15	1.5-15	1.5-15	1.5-15	1.5-15
6	0.3-15	1.5-15	1.5-15	1.5-15	1.5-15
12	0.3-15	1.5-15	1.5-15	1.5-15	1.5-15
18	0.45-15	1.5-15	1.5-15	1.5-15	1.5-15
24	0.6, 1.5-15	1.5-15	1.5-15	1.5-15	1.5-15
30	1.5-15	1.5-15	1.5-15	1.5-15	1.5-15
36	1.5-15	1.5-15	0.075, 1.5-15	0.15, 1.5-15	0.225, 1.5-15
42	2.25-15	1.5-15	0.075, 1.5-15	0.15, 0.675-15	0.15-0.225, 1.5-15
48	3.75-15	0.03, 1.5-15	0.0525-0.675, 1.5-15	0.075-0.225, 1.5-15	0.15-0.3, 1.5-15
54	3.75-15	0.03-0.06, 1.5-15	0.0375-0.15, 0.675-15	0.0675-0.225, 1.5-15	0.15-0.3, 1.5-15
60	5.25-15	0.03-0.0675, 1.5-15	0.045-0.15, 0.675-15	0.0675-0.3, 1.5-15	0.15-0.375, 1.5-15
66	15	0.0225-0.075, 2.25-15	0.0375-0.15, 0.675-0.75, 3-15	0.06-0.3, 2.25-15	0.15-0.375, 2.25-15
72	5.25-15	0.015-0.075, 1.5-15	0.0375-0.225, 0.75, 2.25, 15	0.06-0.3, 6.75-15	0.15-0.375, 6-15
78	0.0075, 5.25-15	0.015-0.075, 0.675-15	0.03-0.225, 1.5-15	0.06-0.3	0.15-0.45
84	0.0075, 5.25-15	0.015-0.075, 0.6-15	0.03-0.225, 1.5-15	0.0525-0.3, 3-15	0.15-0.45
90	1.5-15	0.015-0.075, 0.6-15	0.03-0.225, 1.5-15	0.0525-0.375, 3-15	0.15-0.45
96	0.75-15	0.015-0.075, 0.6-15	0.03-0.225, 1.5-15	0.0525-0.3, 3.75-15	0.15-0.45
102	0.0075, 0.75-15	0.015-0.075, 0.525-15	0.03-0.225, 1.5-15	0.0525-0.3	0.15-0.45
108	0.375, 0.525-15	0.015-0.075, 0.525-15	0.0375-0.15, 0.75-3, 6.75-15	0.06-0.3, 6.75-15	0.15-0.45, 5
114	0.375-15	0.015-0.0675, 0.525-15	0.0375-0.15, 0.675-0.75, 2.25-15	0.06-0.3, 2.25-15	0.15-0.375, 3-15
120	0.525-15	0.0225-0.06, 0.525-15	0.0375-0.15, 0.6-15	0.0675-0.3, 1.5-15	0.15-0.375, 2.25-15
126	0.375-15	0.0225-0.0525, 0.525-15	0.045-0.15, 0.6-15	0.0675-0.225, 1.5-15	0.15-0.375, 1.5-15
132	0.6-15	0.75-15	0.045-0.075, 0.6-15	0.075-0.225, 0.75-15	0.15-0.3, 1.5-15
138	0.75-15	0.675-15	0.045-0.075, 1.5-15	0.075-0.15, 0.675-15	0.15-0.225, 1.5-15
144	3.0-15	1.5-15	0.0525-0.0675, 0.75-15	0.675-15	0.15-0.225, 1.5-15
150	15	1.5-15	1.5-15	1.5-15	0.75-15
156	1.5, 5.25-15	1.5-15	1.5-15	1.5-15	1.5-15
162	2.25-15	1.5-15	1.5-15	1.5-15	1.5-15
168	2.25-15	2.25-15	1.5-15	1.5-15	1.5-15
174	2.25-15	2.25-15	1.5-15	1.5-15	1.5-15

Table 3. Range of stable natural satellite diameters for semi-major axes 6-25 km.

	Semi-major axis (km)					
	6	8	10	15	20	25
i°	Diameter (m)					
0	1.5-15	1.5-15	1.5-15	1.5-15	2.25-15	6-7.5
6	1.5-15	1.5-15	1.5-15	1.5-15	3.0-15	6-6.75
12	1.5-15	1.5-15	1.5-15	1.5-15	2.25-15	6.75, 15
18	1.5-15	1.5-15	1.5-15	1.5-15	3.0-15	6.0-15
24	1.5-15	1.5-15	1.5-15	1.5-15	2.25-15	-
30	1.5-15	1.5-15	1.5-15	1.5-15	2.25-15	-
36	1.5-15	1.5-15	1.5-15	2.25-15	2.25-3, 5.25-6, 15	-
42	0.225-0.3, 1.5-15	0.3, 1.5-15	1.5-15	1.5-15	3	-
48	0.225-0.375, 1.5-15	0.3-0.45, 1.5-15	0.45, 1.5-15	1.5-15	5.25	-
54	0.15-0.375, 1.5-15	0.3-0.525, 1.5-15	0.45-0.525, 1.5-15	2.25-15	-	-
60	0.15-0.45, 2.25-15	0.3-0.525, 2.25-15	0.45-0.6, 2.25-15	2.25-7.5	-	-
66	0.15-0.45, 3-15	0.3-0.6, 3-15	0.45-0.675, 3-15	3, 5.25-6, 7.5-15	-	-
72	0.15-0.45, 4.5, 6.75-15	0.225-0.6, 6.75, 15	0.375-0.675, 4.5-15	3.75	-	-
78	0.15-0.525	0.225-0.6	0.375-0.675	-	-	-
84	0.15-0.525	0.225-0.6	0.375-0.75	-	-	-
90	0.15-0.525	0.225-0.6	0.45-0.75	-	-	-
96	0.15-0.525	0.225-0.6	0.45-0.75	-	-	-
102	0.15-0.525	0.3-0.675	0.525-0.75	-	-	-
108	0.15-0.525, 7.5-15	0.3-0.6, 15	0.6-0.75	-	-	-
114	0.15-0.45, 5.25-15	0.3-0.6, 6.75, 15	0.6-0.75, 15	-	-	-
120	0.15-0.45, 2.25-15	0.375-0.6, 4.5-15	0.675-0.75, 5.25-15	-	-	-
126	0.225, 0.45, 2.25-15	0.375-0.6, 3-15	0.675, 4.5-15	-	-	-
132	0.225-0.375, 1.5-15	0.375-0.525, 2.25-15	3.0-15	15	-	-
138	0.225-0.3, 1.5-15	0.375-0.45, 2.25-15	3-6.75, 15	7.5-15	-	-
144	0.225, 1.5-15	2.25-15	2.25-4.5, 6.75-15	6.75-15	-	-
150	1.5-15	2.25-15	3-4.5, 6-15	6.0-15	-	-
156	1.5-15	2.25-15	2.25-3, 4.5-15	6.0-15	-	-
162	1.5-15	2.25-3.75, 5.25-15	2.25-3, 5.25-15	5.25-15	-	-
168	1.5-15	2.25-15	2.25-3, 5.25-15	5.25-15	-	-
174	1.5-15	2.25-15	2.25-3, 5.25-15	5.25-15	-	-

Progression of Stability with varying size of natural satellite

The data were analyzed by observing the evolution of stable and unstable orbits at a given semi-major axis and increasing the size of the natural satellite. These results can be viewed in Figure 2, where there is 12 graphs that represent the varying initial conditions. Each data point represents an inclination and a longitude of ascending node at a specific time in any given orbit. The sum of all the data yields information on which orbital regions are stable/unstable or if longitude of periapsis precesses $360°$ or less. It should be noted that the color of the data depicts how long the orbit existed before escape of collision. In Figure 2l, there is a color map that can be used to determine the length of time the orbit was stable, where red shows it became unstable in less than 200 years and blue shows it remained stable till the end of the simulation at 1000 years. The first noticeable observations from Figure 2 is that graphs a, b, and c have stable orbits at inclinations between $50° - 100°$, but graphs d-l are unstable in this region. Graphs a-c are stable in this region due to the Sun-terminator plane while the instability in the subsequent graphs are due to instability from the Kozai resonance. This will be discussed in the subsequent sections.The second noticeable features of graphs d-l are the stable regions at low prograde and high retrograde inclinations that do not precess $360°$ through Ω, but rather oscillate around $\Omega = 0°$ or $\Omega = 180°$. These points of stability are the modified Laplace plane orbits. The modified Laplace plane is a frozen orbit in both longitude of periapsis and inclination. Due to short-term perturbations not modeled in the averaged equations of motion, even if the initial conditions were exactly at the modified Laplace plane the orbit would still oscillate. Also, initial conditions that are close to the modified Laplace plane will also oscillate around the stable region, but with larger variance in the inclination and Ω. Further discussion on the modified Laplace plane is in a more detailed section below.

Range of Sizes possible for a Natural Satellite and the Terminator Plane

Table 4. Terminator Plane orbits for objects less than 0.75 m

Semi-major axis (km)	Range of diameters of natural satellite (m)	Mean rate of Ω precession (degrees/year)
2	0.015 - 0.075	305.0516
3	0.03 - 0.225	300.9705
4	0.0525 - 0.75	300.9704
5	0.15 - 0.45	300.8139
6	0.15 - 0.525	300.5749
7	0.15 - 0.6	300.8833
8	0.225 - 0.675	293.223
9	0.3 - 0.675	281.5925
10	0.375 - 0.75	272.0551
11	0.45 - 0.75	256.3294
12	0.675-0.75	241.5403
13	0.75	223.6862

As stated above, it is known that there are no natural satellites orbiting Bennu that is greater than 15 meters in diameter. So the focus of these results were to determine the minimum stable orbits that could exist around Bennu. An example is at 4 km, where the minimum sized stable natural satellite is 5.25 cm. This object was stable for 1000 years at a semi-major axis of 4 km, $\Omega = 0°$, and $i = 90°\ , 96°\ , 102°\ , 108°$. Some Keplerian orbital elements for these 4 orbits can be seen in Figure 3. The semi-major axis, eccentricity, and inclination stay relatively constant for the 1000 year period. Longitude of the ascending node precesses a full 360 degrees. These results have the properties of a terminator plane orbit. In Figure 4, the data for the four different orbits all have a

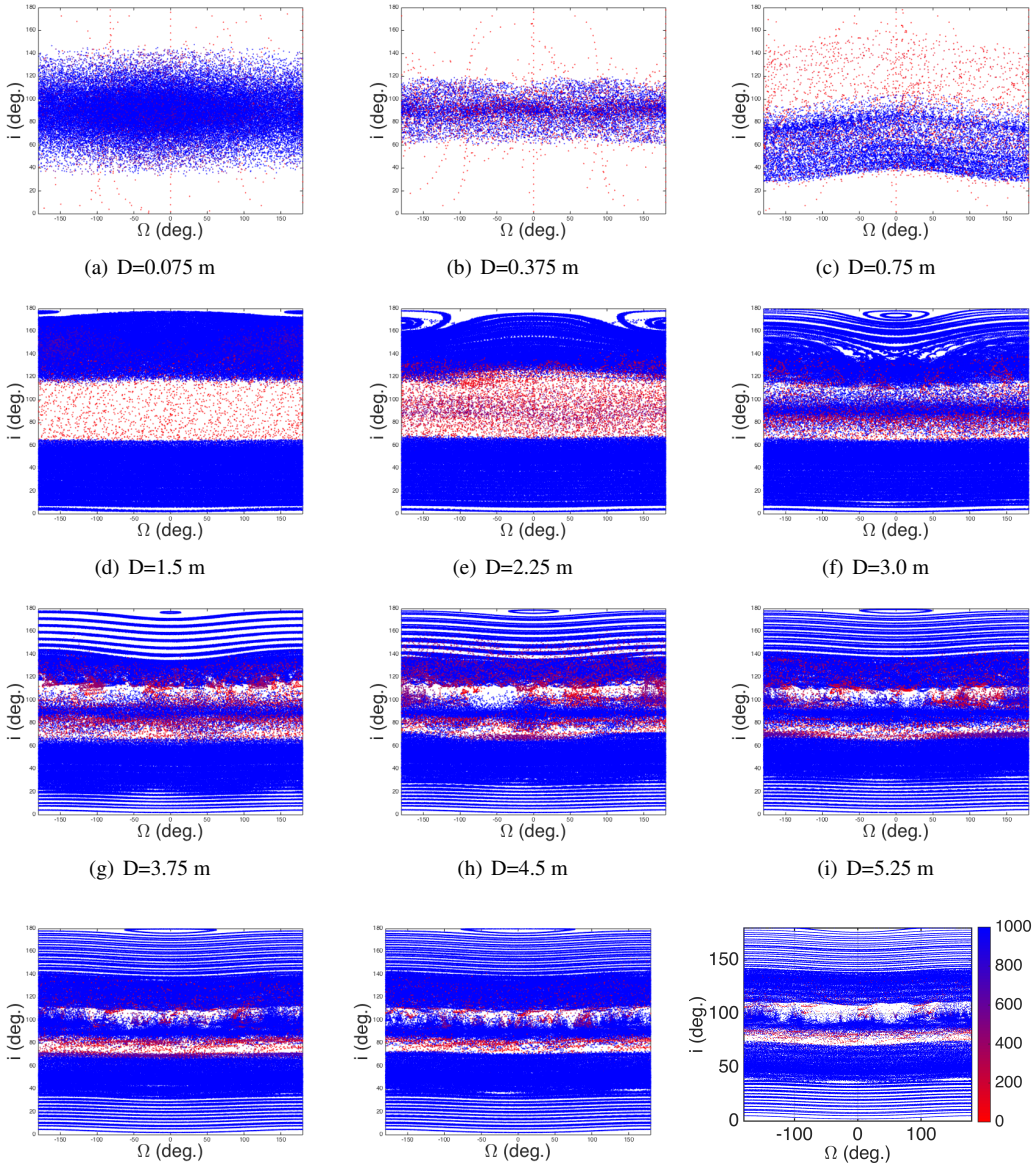

(a) D=0.075 m (b) D=0.375 m (c) D=0.75 m

(d) D=1.5 m (e) D=2.25 m (f) D=3.0 m

(g) D=3.75 m (h) D=4.5 m (i) D=5.25 m

(j) D=6.0 m (k) D=6.75 m (l) D=7.5 m

Figure 2. These 12 figures show the numerical results in blue to red. These figures are in the asteroid-orbit frame at a semi-major axis of 4 km. Each plot above shows the evolution of the inclination versus the longitude of the ascending node over time for increasingly larger natural satellites; starting with Plot A having a diameter of 0.075 m to Plot l representing a 7.5 m diameter object. Each data point is part of an orbit with varying initial conditions. Orbits lasting 1000 years are in blue, while the initial conditions that ended prior to the 1000 years due to escape or collision are in red. Plot l gives the colors that represent how many years before collision/escape for each orbit.

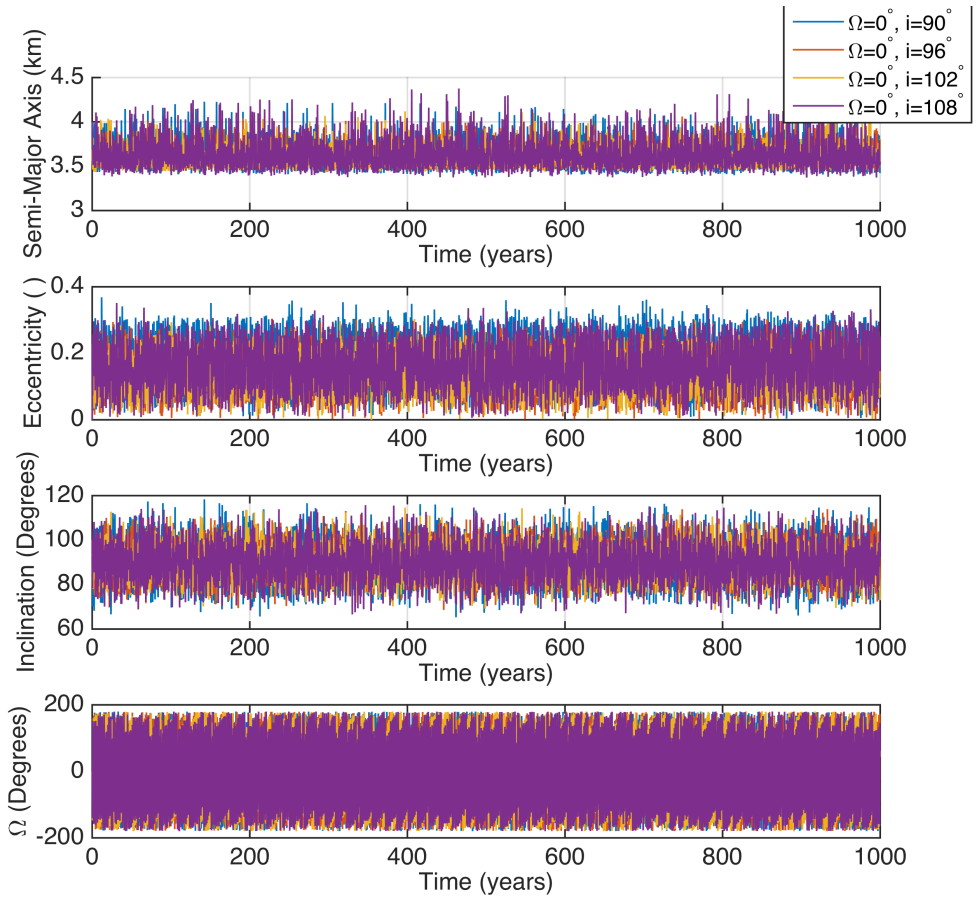

Figure 3. Above is the semi-major axis, eccentricity, inclination and longitude of ascending node for the 4 stable orbits for a 5.25 cm satellite at 4 km.

precession that is similar to the rate of Bennu traveling around the Sun. In fact, the precession rate of each orbit it approximately $300.97°$ which is very similar to Bennu's rate of precession around the Sun of $300.93°$.

The terminator plane for objects smaller that 0.75 m existed for a range from 2 km to 13 km. However, as the semi-major axis increased, the rate of precession for Ω decreased. At 13 km, the precession rate was as slow as $223°$. Therefore, with enough time, these orbits may become unstable. To compare, both $a = 4\ km$ with a 5.75 cm natural satellite and $a = 11\ km$ with a 0.45 m natural satellite were integrated for 10,000 years. It was found that the $a = 4\ km$ orbit was stable after 10,000 years, but the $a = 11\ km$ orbit was no longer stable for that time period. In Table 4, one can view the minimum sized satellite for each semi-major axis that had a stable terminator plane for 1000 years. The rates of precession for semi-major axes 3-7 km will stay stable for 10,000 years, however the larger semi-major axes have reduced precession rates that may become unstable eventually.

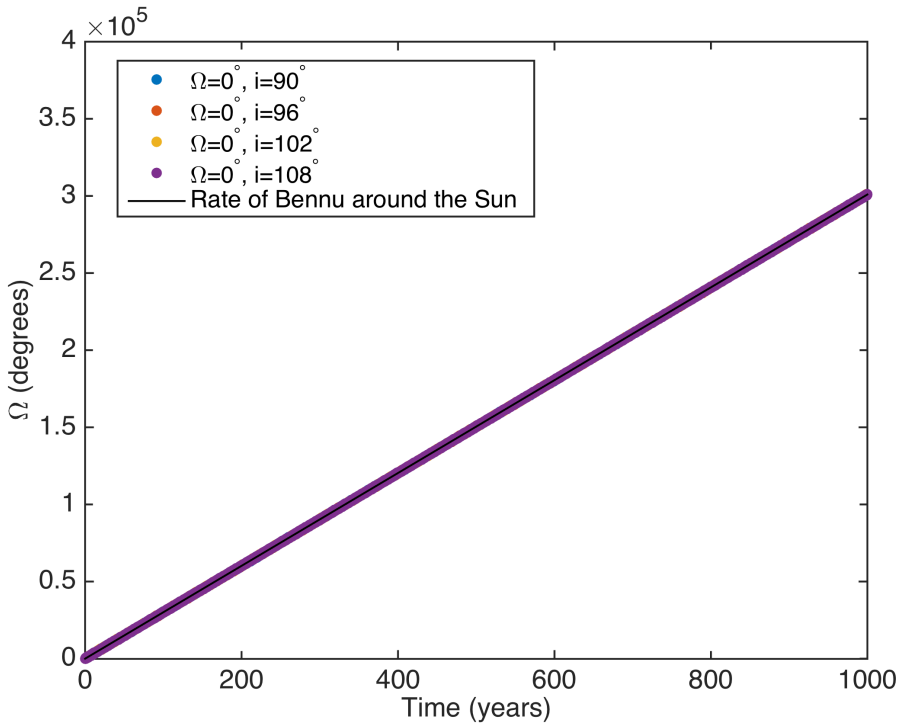

Figure 4. This plot gives a comparison of rate of precession of the longitude of the ascending node of the satellite and Bennu's orbit around the Sun for a 5.25 cm satellite at 4 km. The data for the four different orbits all have a precession that is similar to the rate of Bennu traveling around the Sun.

Stability with the modified Laplace plane

As stated in a previous section, the stable points near $0°$ and $180°$ Ω are most likely the results of the modified Laplace plane due to the lack of precession in the longitude of the ascending node. A way to confirm this is by comparing the averaged equations to the numerical results. We compared the results for $a = 5\ km,\ D = 7.5\ m$ which can be seen in Figure 5. in Figure 5b, just the modified Laplace plane and two other orbits are plotted. In green are the averaged equations of motions results. There is a point at $\Omega = 0°,\ i = 3°$, which is the modified Laplace plane equilibrium, the other two orbits are close enough to the equilibrium that they oscillate around it. In blue are the numerical results. The numerical result for the modified Laplace plane isn't a point but rather a tight circle with some variance in Ω and inclination. Also, the two neighboring orbits also deviate from the averaged equations and have a larger variance in Ω and inclination as well. This is expected because the numerical solutions have perturbations that are not modeled with the secular averaged equations of motion.

Kozai Resonance

The Kozai resonance is determined with averaged equations that only include third body dynamics. In order for the Kozai resonance to occur, the semi-major axis needs to be far enough

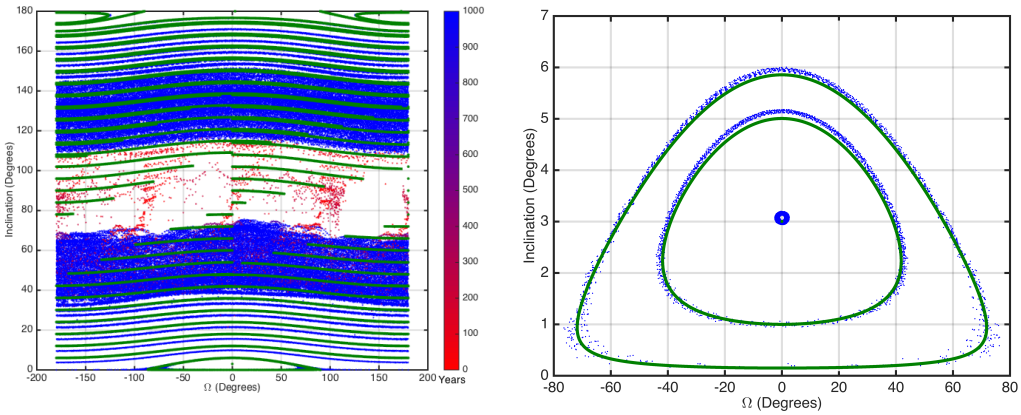

(a) All results

(b) Prograde Modified Laplace Plane

Figure 5. Inclination vs. longitude of the ascending node for $a = 5\ km,\ D = 7.5\ m$ for 1000 years. The orbits that existed 1000 years are in blue, while the initial conditions that ended prior to the 1000 years due to escape or collision are in red. In green are the averaged equations of motion results. In graph a the whole solution set is compared to the averaged equations, but in graph b just the modified Laplace plane and a few other orbits are shown.

away from Bennu that perturbations due to J_2 is no longer significant. Plus, the satellite has to be large enough in diameter such that SRP is no longer a dominating force. Therefore, to determine the possibility of a Kozai resonance around Bennu, the example we used is both far from Bennu at 10 km and a large satellite at 7.5 m in diameter. In Figure 6, there is a plot of eccentricity as a function of inclination. The numerical results for the orbit of one initial condition at $a = 10\ km,\ D = 7.5\ m,\ \Omega = 0°,\ i = 66°$ is given by the blue data points. The general trend of the data is as eccentricity increases, the inclination decreases, which is a property of the Kozai resonance. However, we need to prove the relationship is equivalent to that given in Equation (21). Since, we are using numerical results of an orbit with multiple perturbations on it, we cannot assume L_z or the angular momentum in the $z-$component of the Bennu-Sun orbit plane is constant. Therefore for the value of L_z, we took the mean of all the data points of L_z. Then we used a range of eccentricity from 0 to 0.8 and solved for the inclination. These results are show in Figure 6 as red stars. The numerical data appears to follow the same curve as the analytical Kozai resonance equation. But, there is a much larger variance in the inclination for a given eccentricity in the numerical results. This may be due to the other perturbative forces on the satellite or third body perturbations not accounted for in the averaged equations. Further research will need to be done to verify that this large variation is acceptable and that the orbit can be considered stable for longer periods of time.

The Kozai resonance may also be responsible for the instability regions in Figure 2d-l. The Kozai resonance has a maximum eccentricity value for a given inclination. This relationship is:

$$e_{max} = \left(1 - \frac{5}{3}\cos^2 i\right)^{1/2} \tag{28}$$

For the example orbit with an initial inclination of 66°, the maximum eccentricity is 0.85. Also, the resulting eccentricity from the numerical data never appear to go beyond 0.8. However, as

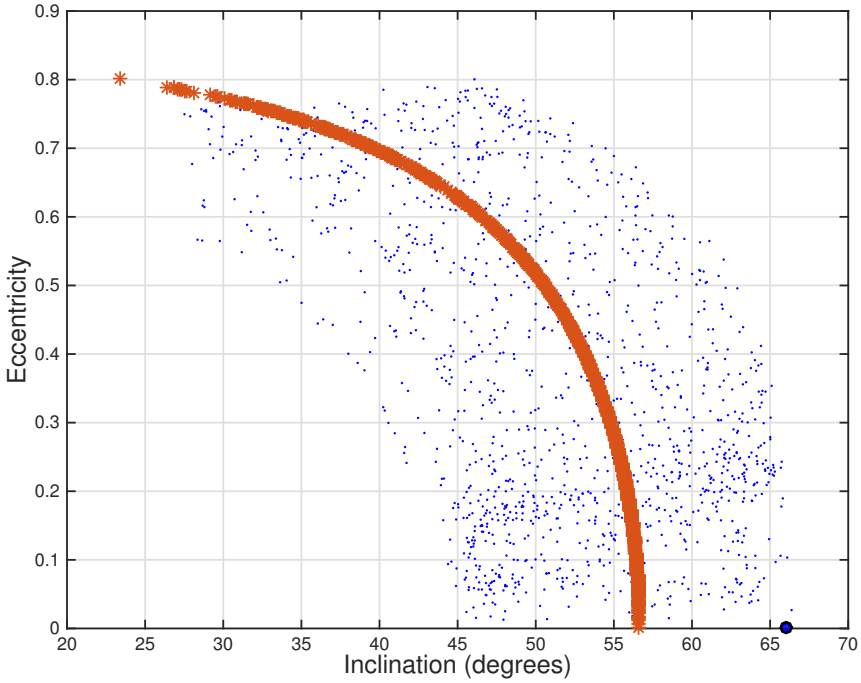

Figure 6. The blue data points are the eccentricity as a function of inclination for the numerical equations of motion for initial conditions of $a = 10\ km,\ D = 7.5\ m, \Omega = 0^\circ,\ i = 66^\circ$. The red data is given by the analytical equation between eccentricity and inclination for the Kozai resonance.

the initial inclination increases, the maximum eccentricity achieved by the Kozai resonance also increases. Eventually, the eccentricity can become so high that the satellite may escape to the Hill sphere or collide with Bennu. Above an inclination of 66°, there is a critical inclination where the eccentricity will eventually become large enough to cause instability through the Kozai resonance. The same case may exist for retrograde orbits as the orbital inclination approaches the equator, the Kozai resonance may become stable again as the maximum eccentricity decreases. This would give the band of instability between $70^\circ - 120^\circ$.

By looking at Figure 2g-l, there exists stable orbits in the region that are supposed to be unstable due to the Kozai resonance. This could be because the the third-body dynamics causing the Kozai resonance is not the only perturbing force or because the simulation did not run for a long enough time to witness the escape/collision that inevitably happens in this region. To see if this is the case, Figure 2i with initial conditions $a = 4\ km,\ D = 5.25\ m$ is ran for 10,000 years. The results are in Figure 7. After 10,000 years all orbits in the $70^\circ - 120^\circ$ range are unstable, which suggests the Kozai resonance may be the reason for this unstable region. f

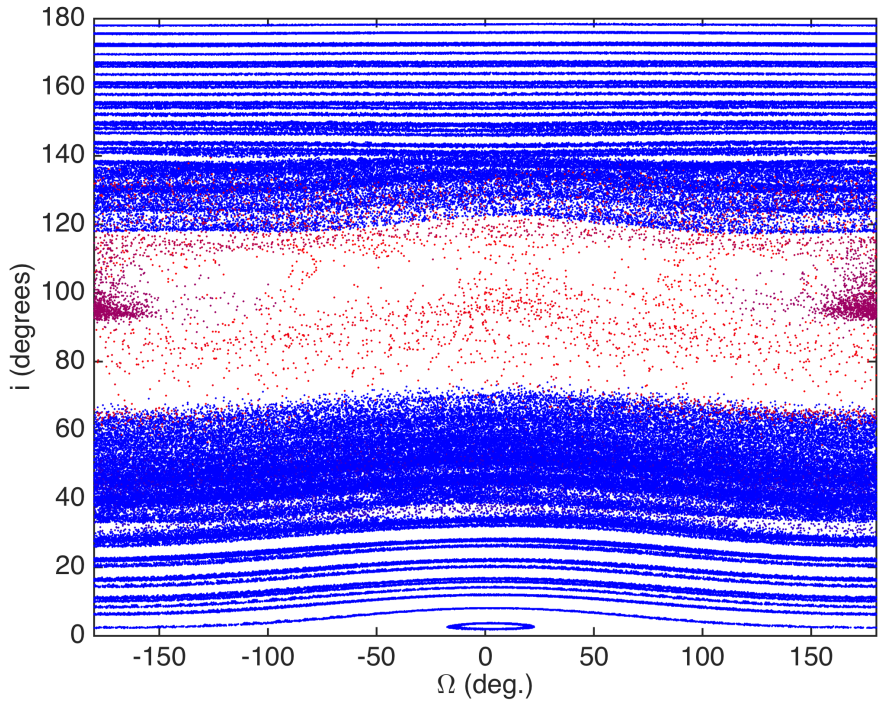

Figure 7. Inclination vs. longitude of the ascending node for $a = 4\ km,\ D = 5.25\ m$ for 10,000 years. The orbits that lasted the 10,000 years are in blue, while the initial conditions that ended prior to the 10,000 years due to escape or collision are in red.

CONCLUSION

Data was collected for possible natural satellites from 0.0075 m. to 15 m at semi-major axes from 1 km to the Hill sphere. The 120 iterations vary with $\Omega = 0^\circ\ , 90^\circ\ , 180^\circ\ , 270^\circ$ and inclination from 0° to 180° in increments of 6 degrees. An example of the data were given to show how the stable and unstable orbits evolved as the size of the natural satellite increased at a constant semi-major axis. Multiple observations were made on whether the Sun-Terminator plane, modified Laplace plane and Kozai resonance could be use to help understand certain regions. The Sun-terminator plane was found to be the orbit where smaller sized natural satellites exist. The terminator plane was determined to be the reason for this orbit due to the rate of precession of the longitude of the ascending node being equivalent to the rate of Bennu's orbit around the Sun. The terminator plane was the orbit for the smallest natural satellites at 2-13 km. However from 8-13 km, the rate of precession was lower, and will eventually cause the orbits to become unstable. The stable points near 0° and 180° Ω are due to the modified Laplace plane. These equilibrium points existed for diameters from 1.5 m to 15 m. Finally the Kozai resonance may be responsible for stable orbits of large or far away objects that precess 360° through the longitude of the ascending node. This was determined by comparing an analytical equation for the Kozai resonance that represents the exchange between inclination and eccentricity to the numerical results. Finally, the Kozai resonance may also be responsible for the unstable region for inclinations from $70^\circ - 120^\circ$. In this region, the Kozai

resonance reaches very high eccentricities that causes the satellites to eventually collide or escape. This is further supported by evidence that when the initial conditions for $a = 4\ km,\ D = 5.25\ m$ was integrated for 10,000 years as opposed to 1000 years, the entire region eventually became unstable.

Future Work

So far there has been some examples on what may be causing these stable and unstable regions, however the data has not been fully characterized. There is one example of the Kozai resonance occurring at $a = 10\ km,\ D = 7.5\ m, \Omega = 0°,\ i = 66°$, however it is not understood what range of diameters the natural satellite or distance from Bennu that the Kozai resonance occurs. Also, Bennu is an asteroid with a complex gravity field that is not well represented by modeling just J_2. Therefore the next step is to further compute the gravity field with more spherical harmonics to help determine how this effects the stability of these orbits. Lastly, just because a satellite can exist in a certain orbit, does not mean that one will actually be there. The final step is to understand how possible satellites would settle into these orbits.

REFERENCES

[1] C. Hergenrother, M. Barucci, O. Barnouin et al., "The Design Reference Asteroid for the OSIRIS-REx Mission Target (101955) Bennu", 2014.

[2] Y. Kozai, "Secualar Perturbations of Asteroids with High Inclination and Eccentricity," *The Astronomical Journal*", vol. 67, Issue 9, 1962, pp. 591-598.

[3] D. S. Lauretta, et. al., "The OSIRIS-REx target asteroid (101955) Bennu: Constraints on its physical, geological, and dynamical nature from astronomical observations," *The Meteoritical Society*, vol. 50, July 2014, p. 834-839.

[4] M. C. Nolan, et. al., "Shape model and surface properties of the OSIRIS-REx target Asteroid (101955) Bennu from radar and lightcurve observations", *Icarus*, vol.226, May 2013, p. 629-640.

[5] M. Nolan, C. Magri, E. Howell et al., "Shape model and surface properties of the OSIRIS-REx target Asteroid (101955) Bennu from radar and lightcurve observations," *Icarus*, Vol. 226, Issue 1, 2013, pp. 629-640.

[6] S. M. Rieger, and Scheeres, D. J., "Laplace Plane Dynamics with Solar Radiation Pressure in the Vicinity of an Asteroid," AIAA/AAS Astrodynamics Specialists Conference, San Diego, CA, August 7, 2014.

[7] A. J. Rosengren, and D. J. Scheeres, "Laplace Plane Modifications Arising From Solar Radiation Pressure," *The Astrophysical Journal*, vol. 786, May 2014, p. 45.

[8] A. J. Rosengren, and D. J Scheeres, "On the Milankovitch orbital elements for perturbed Keplerian motion," *Celestial Mechanics and Dynamical Astronomy*, vol. 118, Jan. 2014, pp. 197220.

[9] A. J. Rosengren, D. J. Scheeres, and J. W. McMahon, "The classical Laplace plane as a stable disposal orbit for geostationary satellites," *Advances in Space Research*, vol. 53, Apr. 2014, pp. 12191228.

[10] D. J. Scheeres, "Orbit Mechanics About Asteroids and Comets," *Journal of Guidance, Control, and Dynamics*, vol. 35, May 2012, pp. 987997.

[11] D. J. Scheeres, ,"Orbital Motion in Strongly Perturbed Environments: Applications to Asteroid, Comet and Planetary Satellite Orbiters", Springer in Association with Praxis, Heidelberg, 2012. p3-11, 255-275

[12] S. Tremaine, J. Touma, and F. Namouni, "Satellite Dynamics on the Laplace Surface," *The Astronomical Journal*, vol. 137, Mar. 2009, pp. 37063717.